The Perceived Roughness of Resistive Virtual Textures: I. Rendering by a Force-Feedback Mouse

ROBERTA L. KLATZKY
Carnegie Mellon University
and
SUSAN J. LEDERMAN
Queen's University

In previous work, we demonstrated that people reliably perceive variations in surface roughness when textured surfaces are explored with a rigid link between the surface and the skin [e.g., Klatzky and Lederman 1999; Klatzky et al. 2003]. Parallel experiments here investigated the potential of a force-feedback mouse to render surfaces varying in roughness. The stimuli were surfaces with alternating regions of high and low resistance to movement in the x (frontal) dimension (called ridges and grooves, respectively). Experiment 1 showed that magnitude ratings of roughness varied systematically with the spatial period of the resistance variation. Experiments 2 and 3 used a factorial design to disentangle the contributions of ridge and groove width. The stimuli constituted eight values of groove width at each of five levels of ridge width (Experiment 2) or the reverse (Experiment 3). Roughness magnitude increased with ridge width while remaining essentially invariant over groove width. Kinematic variations in exploration were observed across the surfaces. The data point to the promise of using inexpensive devices to create virtual textural variations under conditions of unconstrained exploration.

Categories and Subject Descriptors: H.5.1 [**Information Systems**]: Information Interfaces and Presentation—*Multimedia information systems*; H.5.2 [**Information Systems**]: Information Interfaces and Presentation—*User interfaces*

General Terms: Artificial, Augmented, and Virtual Realities, Evaluation/Methodology; Ergonomics, Haptics I/O, User-Centered Design, Human Factors

Additional Key Words and Phrases: Texture perception, virtual reality, haptics

1. INTRODUCTION

When people touch a textured surface, one of the most salient perceptual aspects is its roughness. The study of roughness perception through the haptic system has, accordingly, received considerable attention from psychophysicists, neurophysiologists, and computational theorists. Until recently, this work has focused on the perception of roughness via direct contact between the skin and the textured surface, as occurs when we rub a surface with a finger. In this paper, we present psychophysical results describing texture perception through a different medium, namely, a force-feedback computer mouse, the WingMan (Logitech). The textures were formed by regions with alternating resistance values, where resistance resulted from friction and viscosity. To the extent that the surfaces that are rendered by the mouse produce different degrees of perceived roughness, this technique has potential for broad,

---

Authors' addresses: Roberta L. Klatzky, Department of Psychology, Carnegie Mellon University, Pittsburgh, PA 15213; Susan J. Lederman, Department of Psychology, Queen's University, Kingston, Ontario K7L 3N6 Canada.

inexpensive application. In a companion paper [Lederman et al. 2006], we systematically explore resistive textures with a more precise, but less affordable, force-feedback interface, the PHANTOM (SensAble), using a viscosity algorithm derived from the present research.

In conducting research with the WingMan mouse, we recognize that it was not intended for highly controlled psychophysical studies. Indeed, anecdotal reports, our own experience, and the device specifications (see below) all indicate that it is limited in repeatability and that the output varies with the position and nature of the display. If, however, despite these limitations, it is possible to obtain regularities in perceived roughness as a function of display manipulations, it would make an even stronger case that inexpensive devices have promise for conveying textural percepts.

Human roughness perception has been tested with systematic psychophysical procedures in three situations—real textures felt with the bare skin, real textures felt through a rigid link, such as a stylus held in the hand, and virtual textures that are rendered by force-feedback devices. The companion paper by Lederman et al. [2006] provides a review of the first two of these situations. To summarize the findings, empirical and theoretical work indicates that roughness perception with the bare skin is coded by both spatial and temporal variations in pressure. The relative importance of spatial and temporal processes appears to vary with the scale of the texture, as determined by the spacing between the elements that form it. Specifically, there is a transition from spatial to temporal coding as the texture becomes finer. When texture is perceived via a rigid link held in the hand, as opposed to via contact with the bare skin, processing responds to variations in pressure resulting from the physical interactions between the rigid interface and the textured surface. In this case, temporal processes necessarily dominate, as the spatial distribution of the pressure on the skin is uncorrelated with the surface variations.

The present review concentrates on the third situation mentioned above, rendered textures. There has been considerable interest in producing virtual textures with haptic force-feedback devices such as the PHANTOM. The present experiments provide analogous results for perception of textures rendered by the force-feedback mouse. Research on virtual textures has been motivated by both basic and applied concerns. Force-feedback devices potentially allow precise control over surface properties with relative ease of fabrication, opening up new basic research possibilities for understanding human somatosensory perception. Moreover, realistic simulated surfaces could be used in many applied contexts. For example, simulated roughness could provide a sense of material properties over the internet for purposes of e-commerce.

Textures have been computationally rendered with a variety of devices and algorithms. One variation is the number of degrees of freedom (DoF) the device has. Minsky [1995]; Minsky and Lederman [1996] generated textures in a two-DoF environment, by generating a tangential (lateral) force proportional to the gradient of the underlying surface/height profile. Fully three-dimensional (3D) algorithms have been applied in a number of studies, using model surfaces generated from a sinusoid or other function [e.g., Choi and Tan 2002, 2003; Colwell et al. 1998; Ho et al. 2004; Massie 1996; Penn et al. 2003a, 2003b]. Otaduy and Lin [2004] modeled the interaction between a probe and a sinusoidal texture ("six-DoF haptics") and compared their results qualitatively to those obtained by Klatzky and Lederman for rigid probes held in the hand [Klatzky and Lederman 1999, 2002; Klatzky et al. 2003; Lederman et al. 1999, 2000]. An alternative to geometric surface models is to apply vibrations based on measurements of real surfaces [Jansson 1998; Okamura et al. 1998; Wall and Harwin 1999]. Siira and Pai [1996] developed a stochastic technique for rendering. They created synthetic textures by generating tangential forces only, or both tangential and normal forces, from a Gaussian distribution and then adding them to nonrandom forces that impose rigidity and friction.

While the simulation of textures remains an exciting frontier, a number of problems have been noted. Campion and Hayward [2005] provided a set of criteria for evaluating limits on the rendering of textures. The criteria are, to some extent, heuristic, as they incorporate "safety factors" that can vary over a sizeable range. Their tests on a PHANTOM Premium1.0A indicated a surprising level of distortion at gratings as large as 10 mm. Others have documented buzzing or humming in the rendering device at critical frequencies [Choi and Tan 2002, 2003]. The calculation of collision forces to create forces transmitted to the hand is computationally demanding [Siira and Pai 1996]. Another important consideration is that haptic devices remain, for the most part, costly for broad access and application. Moreover, detailed psychophysical evaluation for texture algorithms has not been extensive.

Several evaluation studies have used ratings of roughness to assess the quality of virtual textures. Minsky and Lederman [1996] used a magnitude-estimation procedure to determine how perceived roughness was determined by force amplitude and geometric parameters of the display. Using a PHANTOM, Penn and colleagues [Penn et al. 2003a, 2000b] examined roughness magnitude as a function of groove width in sinusoidal virtual textures and found a monotonic decreasing function. One explanation of this result is that the PHANTOM, which simulates a point contact, acts like a probe with an infinitely small tip. As spacing increases, such a probe will ride for longer distances without encountering disrupting forces; hence, the magnitude-estimation function should be decreasing. A similar result was found by Colwell et al. [1998] with a different device. Also consistent with the previous results, Drewing et al. [2004] examined roughness ratings of jittered raised-dot patterns generated with the PHANTOM and found that roughness ratings could not be discriminated from those of spatial density. In contrast, again with the PHANTOM, but with sandpaper-like displays, Jansson [1998] found that roughness increased with interelement spacing, although spacing and element size were correlated in that study.

A variety of other methods for evaluating simulated textures have been used. Minsky [1995] used ratings of confidence that a texture was present. Using relatively informal documentation, Siira and Pai [1996] assessed their stochastically generated textures as realistic in feeling, although the tangential forces alone were found unsuitable for coarse textures. Other psychophysical studies using rendered textures have been concerned not with perceived roughness, but with discrimination and matching [e.g., Ho et al. 2004; Wall and Harwin 1999; Weisenberger et al. 2000].

In the present study, we systematically evaluated the utility of an inexpensive device for creating a sense of surface roughness. The device is a force-feedback mouse (the WingMan from Logitech). We implemented a one-DoF algorithm that alternates relatively smooth and resistant patches. Standard psychophysical techniques were used to determine not only whether a consistent and coherent sense of roughness could be conveyed, but what parameters governed it and over what range of variation. The psychophysical outcome from resistance-based roughness can be compared to outcomes from other studies that assess vibratory roughness by using rigid links, as well as to psychophysical work using force-feedback devices.

2. GENERAL METHOD

2.1 The WingMan Mouse

The haptic stimuli were textured surfaces presented by means of the WingMan mouse, essentially virtual rectangular gratings. It measures 104 mm long by 74 mm wide and is 35 mm high at the apex. It has a range of movement of approximately 2.2 cm in the x direction (across the screen, roughly frontal with respect to the user) and 1.8 cm in the y direction (up the screen, roughly sagittal with respect to the user). Further movement is prevented by a tether that links the mouse to the pad. The mass is approximately 0.12 kg. We calibrated the position resolution in x as 51 pixels/mm and that conversion is used in the present paper. The following are approximate specifications obtained from the designers (personal communication, 2005): position resolution of about 1200 counts in actuator space (roughly on the diagonal of the screen/mouse workspace); nominal maximum design force of 1 N in any direction;

10-bit D/A resolution giving ±9 bits of force resolution in each direction; processor with custom 16-bit fixed-point architecture @ 10 MIPS; and internal force loop at 1 kHz with typical effect load, dropping to 500 Hz with complex computations (e.g., textures inside an elliptical boundary).

The space in which the mouse moved was partitioned by a texture algorithm from the Immersion Toolkit into strips that constituted what will be called ridges and grooves, in keeping with the psychophysical literature on texture perception. The strips were oriented so that a ridge or groove projected along the y axis and ridges and grooves alternated across the x axis. Within a strip designated as a ridge, mouse movement along the x axis in either direction was resisted. Based on measurement procedures described in the Appendix, we characterize the resistance within a groove as due to sliding friction only and the resistance within a ridge as including essentially the same sliding friction and adding a viscosity component. The coefficient of sliding friction was measured as approximately 0.5 and, at the resistance-parameter setting we used for ridges (coded by the tool kit as 6000), the viscosity of the ridge was approximately 0.01 N-s/mm (for details, see Appendix).

We evaluated the mouse at a spatial period of 0.08 mm, the smallest used here, relative to the heuristic rendering limits described by Campion and Hayward [2005]. The evaluation was based on the designer specifications above and an assumed velocity of 50 mm/s, the average velocity observed in Experiment 1 for that spatial period. The device proved marginally adequate to render such a fine texture under the tested model. Considering the velocity limit test, if one adopts a safety factor of 2, the smallest suggested by Campion and Hayward, the outcome of 1.25 exceeds the criterion of 1.0. With the minimum safety factors of 2, the tests for speed reconstruction are passed. Force reconstruction appears to be adequate assuming a force amplitude of 0.33 N. (We could not test gain limit or device structural limit.)

2.2 General Design and Procedure

All subjects were right-handed by self-report. The subject was seated in front of the computer visual display. His or her right arm entered a box with a curtain on the front, so that the hand and wrist were not visible. The box was placed so that the mouse was aligned with the subject's shoulder. The right hand grasped the mouse. The subject wore headphones that played white noise at a comfortable level, which was adequate to mask the sounds from surface exploration.

On each trial, the subject felt the surface as long as desired by moving the mouse on the pad, freely within the constraint of the tether. No instructions about movement were provided and subjects did not encounter obvious instabilities. The subject then used the keyboard to enter a magnitude indicating the roughness of the surface, using whole numbers or fractions, but avoiding the response "zero." Because some pilot subjects were uncertain as to how to define roughness with these surfaces, the instructions compared the mouse to a car on a road and asked subjects to think of how rough the road felt. The entered value was displayed on the monitor and could be edited until the next response was made.

The general nature of the design followed work of Lederman [1974, 1983] by employing a stimulus set that allowed effects of potentially critical geometric factors to be systematically evaluated. In each experiment, a set of surfaces was generated by factorially varying one or more of the following parameters: ridge width, groove width, the ridge:groove width ratio, and spatial period (i.e., the sum of ridge and groove widths). There were three replications of the resulting conditions. Within each replication, each surface was presented once, in random order. The experiments that are reported here differed with respect to the parameters that were varied and the range of variation.

To construct the surfaces, given the design parameters, the ridge and groove widths were initially specified in millimeters, then converted to pixels as defined by the mouse, then reconverted to millimeters for report. Because pixels had to be in whole numbers, rounding changed some of the ultimate values. In some cases, with the finest surfaces, two conditions that were intended to be distinct within the design had the same pixel values and were, therefore, consolidated. Below, we specify ridge and groove values in millimeters after the conversion back from pixels. For analysis and exposition, the ridge:groove ratio is given by the ideal value before the conversion, ignoring variations due to the millimeter-to-pixel mapping.

A further constraint on the design of the stimuli was that in pilot testing, subjects found it difficult to judge the roughness of textures that had a ridge:groove ratio exceeding 3.0. With larger ratios, the surfaces felt more resistive than rough. We, therefore, limited ridge:groove ratios to 3.0 or lower.

3. EXPERIMENT 1

The purpose of this initial experiment was to explore roughness responses over a large range of ridge and groove values, varying spatial period and ridge:groove ratio.

3.1 Method

Twelve subjects from the university student population participated. There were seven males, four females, and one subject whose gender was not recorded. The stimulus surfaces were generated by combining eight values of spatial period with five values of ridge:groove ratio. The spatial period values were 0.08, 0.16, 0.29, 0.57, 1.11, 2.15, 4.14, and 7.99 mm. The ridge:groove ratios were 1.00, 0.50, 0.33, 2.00, and 3.00. After consolidating cells of the design due to equivalence from millimeter-pixel conversion, there were 38 distinct surfaces—three ridge:groove ratios at the smallest value of spatial period and five at all other values of spatial period. The size of a ridge or groove thus spanned from 0.04 to 4.00 mm. Note that with this design, the values of both ridge and groove increase with spatial period. In other respects, the method was as described in the general method section.

3.2 Results

The analysis for this and the remaining experiments proceeded as follows. Initially, the roughness magnitudes were averaged over replication. To normalize across variations in subjects use of the magnitude scale, the average was divided by the subject mean and then multiplied by the grand mean to restore overall scale. The log of the normalized value was used in further analyses. Analyses of variance (ANOVAs) were performed according to the design of the given experiment.

Figure 1 shows the log of roughness as a function of log spatial period by ridge:grove ratio. Log perceived roughness was a strongly increasing function of log spatial period at each ridge:groove level. Further, there was substantial overlap among the functions for distinct ridge:groove ratios, but ridge:groove modulated the function to some extent, particularly for the lowest spatial periods. These relationships were confirmed by two ANOVAs. As the experimental design was factorial when the smallest value of spatial period was eliminated, the first ANOVA was performed on the remaining spatial periods with factors ridge:groove ratio (5) and spatial period (7). It showed significant effects of ridge:groove, $F(4, 44) = 7.74, p < 0.0001$, spatial period, $F(6, 66) = 66.17, p < 0.0001$, and the interaction, $F(24, 264) = 1.82$, $p < 0.05$. To further characterize these effects, we evaluated the simple main effect of ridge:groove ratio at each level of spatial period. The effect was significant for spatial periods of 0.16, 0.29, and 0.57 mm, but not thereafter, suggesting that roughness increased with ridge width at low spatial periods, but this effect eventually saturated.

When the three roughness estimates at the smallest value of spatial period (i.e., those not included in the previous two-way ANOVA, seen at the far left of Figure 1) were examined in isolation, the trend was for roughness to increase with ridge:groove ratio, as was found in the main analysis for small spatial periods. The second ANOVA, a one-way across the three conditions, found, however, that the effect of ridge:groove ratio was not significant, $F(2,22) = 1.18$. Note that this spatial period was close to the rendering limits identified by Campion and Hayward [2005].

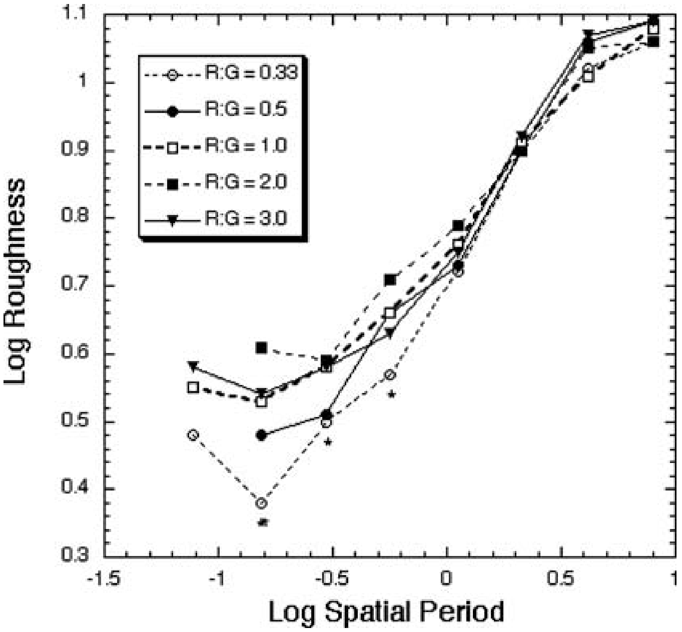

Fig. 1. Perceived roughness (means of the log normalized roughness magnitude estimates) in Expertment 1 as a function of log spatial period, by ridge:groove (R:G) ratio. The asterisks mark spatial periods within which there was a significant effect of ridge:groove ratio.

The overall trends in Figure 1 rule out the ridge:groove ratio per se as a direct determiner of roughness, but there are various possible interpretations of the data, given the design. One is that spatial period predominates in governing perceived roughness, that is, that the scale of the texture is critical. Another is that some other factor that covaries with spatial period underlies the roughness percept. Given the design, this other factor could be either ridge width or groove width (log ridge and log groove widths are correlated in this design, $r(36) = 0.85$ across surfaces). The previous analyses provide more support for the importance of ridge width, at least when spatial period is not large. Moreover, the simple correlation between log roughness and log ridge width [$r(36) = 0.95$] was greater than that between log roughness and log groove width [$r(36) = 0.89$].

Figure 2 plots the log perceived roughness values from Experiment 1 by log ridge width, while grouping similar groove widths into bins. It can be seen, as was indicated by the analyses reported above, that roughness increases with ridge width until it saturates at the highest values. The data from different groove values, holding ridge constant, substantially overlap, suggesting little effect of groove width. To more effectively dis-entangle the effects of ridge and groove width, we performed further experiments in which ridge:groove ratio was factorially varied with ridge width (Experiment 2) or groove width (Experiment 3).

4. EXPERIMENT 2

This experiment was modeled after studies of Klatzky and Lederman [1999], which examined the effects of spacing between raised dots in an otherwise flat surface. In those studies, textures were formed by raised cylindrical elements of a constant diameter, and interelement spacing was varied. The analogy to the current situation is to use a fixed ridge width (analogous to a cylindrical element of fixed diameter) and to vary groove width (analogous to varied interelement spacing). Holding ridge width constant and

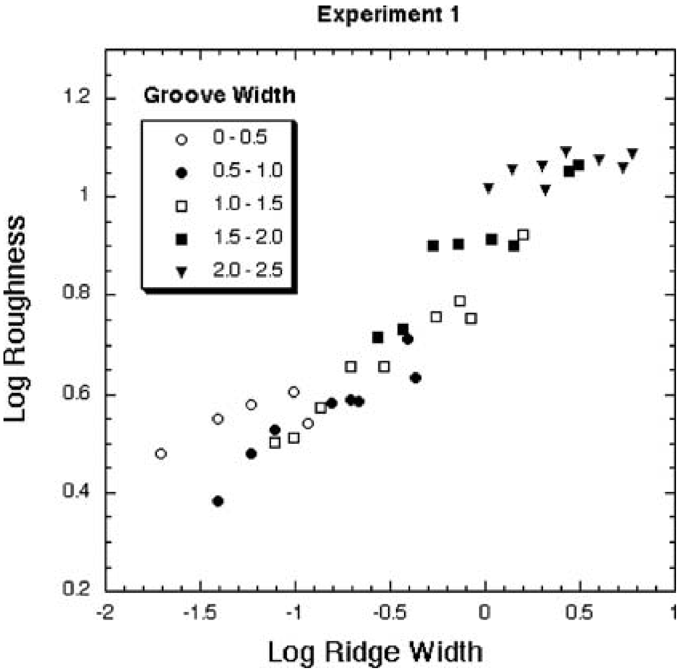

Fig. 2. Perceived roughness (means of the log normalized roughness magnitude estimates) in Experiment 1 as a function of log ridge width (mm), for each of five ranges of groove width (mm).

varying groove means that the ridge:groove ratio varies. The resulting surfaces were replicated at each of five scales, where a scale corresponds to a ridge width.

4.1 Method

Fifteen subjects, nine male and six female, from the university student population participated. The design crossed eight values of ridge:groove ratio—0.22, 0.25, 0.29, 0.35, 0.43, 0.57, 0.82, and 1.50—with five values of ridge width—0.08, 0.16, 0.31, 0.64, and 1.25 mm. The resulting groove widths varied from approximately 0.05 to 5.7 mm. (As noted above, the actually implemented values of ridge:groove ratio depended on nearest pixel equivalents.) In other respects, the method was as described in the general method.

4.2 Results and Discussion

At each of five scales [ridge width values], there were eight values of ridge:groove ratio. An ANOVA on these factors showed significant effects of ridge width, $F(4, 56) = 22.09$, $p < 0.0001$, and the interaction, $F(28, 392) = 3.42$, $p < 0.0001$.

Figure 3 (left panel) shows log roughness as a function of log groove width, with symbols differentiating the different scales (ridge widths). It can be seen that log roughness increased overall with log groove width, but this effect was due to the correlation between ridge and groove width. Indeed, within each value of ridge width, log roughness did not systematically increase with log groove width.

To statistically assess this pattern, we fit linear functions relating log roughness to log groove within each level of ridge width. Figure 4 shows the average slopes and intercepts of these functions, in relation to the same parameters from Experiment 3, which is described below. When 95% confidence intervals around the mean slope were constructed for each scale, only one slope—for scale value 4—was

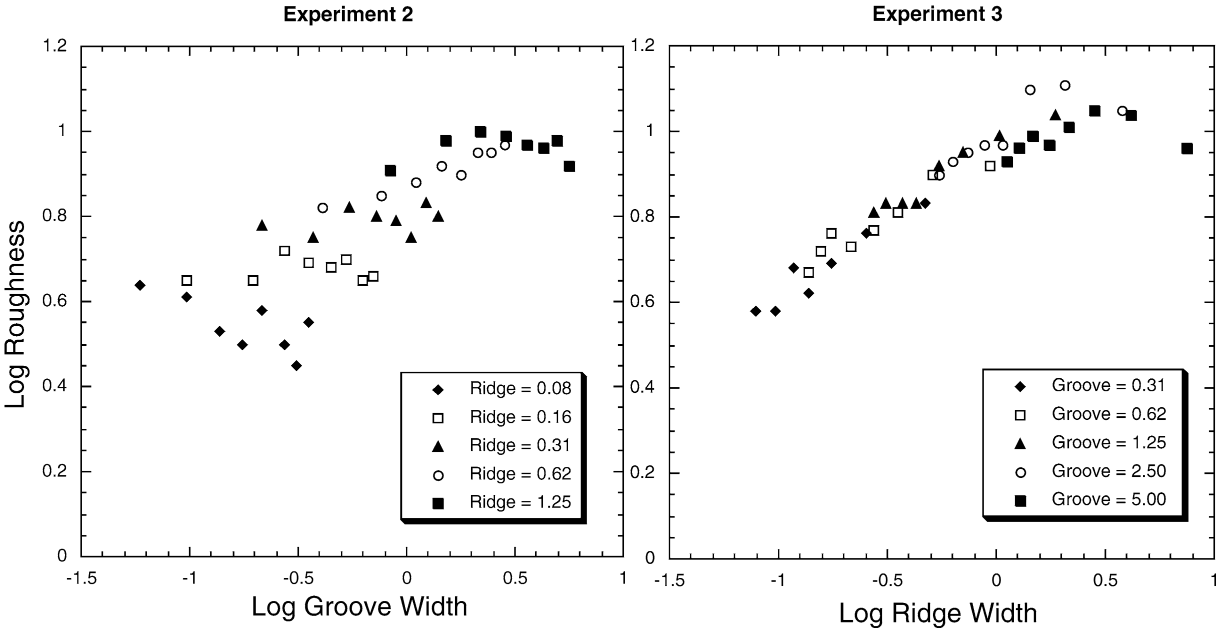

Fig. 3. *Left panel*: Perceived roughness (means of the log normalized roughness magnitude estimates) as a function of log groove width (mm) in Experiment 2, at each level of ridge width (mm). *Right panel*: Perceived roughness as a function of log ridge width (mm) in Experiment 3, at each level of groove width (mm).

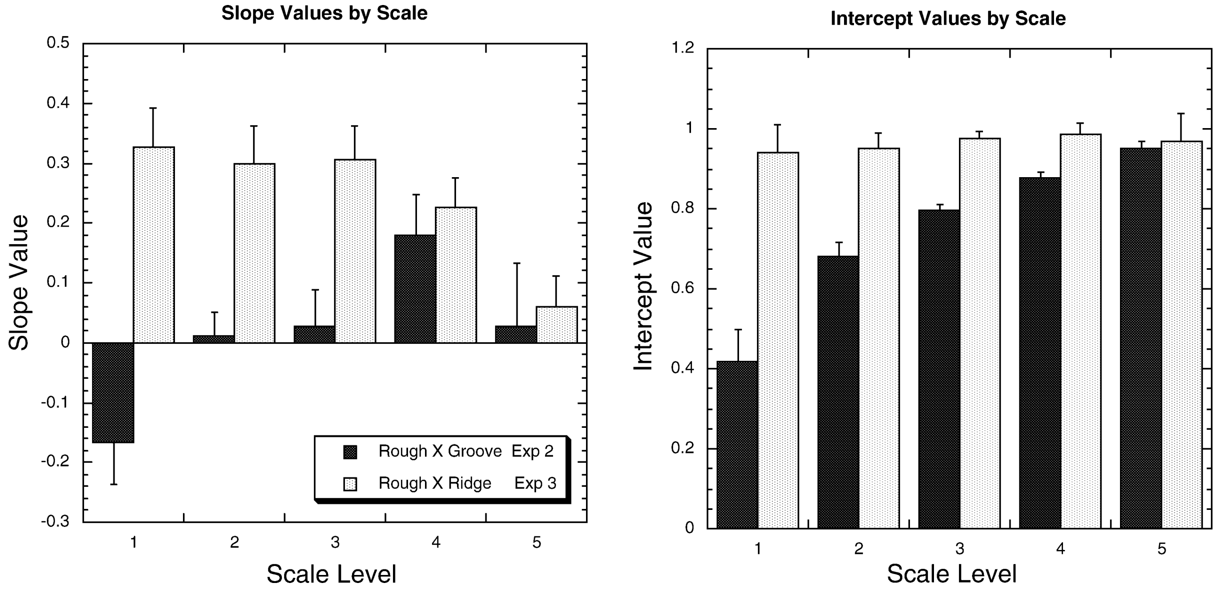

Fig. 4. Slopes (*left panel*) and intercepts (*right panel*) of linear functions relating log perceived roughness (mean of log normalized roughness magnitude estimates) to stimulus parameters, at each of five scales. In Experiment 2 (dark bars), the functions relate log perceived roughness to log groove width and scale corresponds to five levels of ridge width. In Experiment 3 (light bars), the functions are log perceived roughness by log ridge width; scale corresponds to five levels of groove width. Error bars are 1 SEM.

significantly above zero; one of the other slopes was negative. Thus, there was no general tendency for a positive slope, which would have indicated an increase in roughness with groove width.

The intercepts of the same linear functions relating roughness to log groove were all significantly above zero by the confidence-interval test. If roughness is largely determined by ridge width, which increases with scale, the intercepts should also increase with scale. A linear trend analysis confirmed that the intercepts increased with scale, $F(1, 56) = 84.29$, $p < 0.001$. However, it is noticeable that the increase in intercepts is greater across the lower values of scale than the higher ones. Post hoc tests [Fisher's LSD] indicated that the intercept for scales 5 [ridge width = 1.25 mm] and 3 [ridge width = 0.31 mm] differed significantly, but scales 5 and 4 did not. This indicates that the effect of ridge is saturating as ridge width increases, similarly to the saturation observed in Experiment 1.

To summarize, the data from Experiment 2 showed a strong tendency for roughness to increase with ridge width, but not consistently with groove width. Experiment 3 provided a further test of the roughness/ridge relationship by transposing the design of Experiment 2.

5. EXPERIMENT 3

In this experiment, groove width was held constant in order to define a level of scale, and ridge width varied within that scale. This allowed an assessment of the effect of ridge with groove width constant, in contrast to the reverse in Experiment 2.

5.1 Method

Thirteen subjects, eight male and five female, from the university student population participated. To construct the surfaces, five values of groove width—0.31, 0.63, 1.25, 2.50, and 5.00 mm—were crossed with eight values of ridge:groove ratio—0.22, 0.25, 0.29, 0.35, 0.43, 0.57, 0.82, and 1.50. The ridge:groove ratios were the same as in Experiment 2 and the maximum value of groove width (5.0 mm) was also similar to that of Experiment 2 (5.7 mm). The range of ridge values in this experiment (0.07–7.5 mm) was accordingly somewhat larger than the range of groove values in the previous experiment (0.05 mm—5.7 mm). Because there were two combinations of ridge:groove ratio and groove width that yielded the same number of pixels, the observation at ridge:groove = 0.22, groove = 0.31, was eliminated from the design. In other respects, the method was as described in the general method section.

5.2 Results and Discussion

Figure 3 (right panel) shows log roughness as a function of log ridge width at each of the five scales, as defined by groove width. Because of the eliminated cell in the design, we performed separate ANOVAs on the two subdesigns, one eliminating the smallest ridge:groove ratio and one eliminating the smallest groove width. Both ANOVAs showed significant effects of groove width, ridge:groove ratio, and the interaction: For groove, $F(4, 48) = 7.14$ and $F(3, 36) = 4.52$; for ridge:groove, $F(6, 72) = 16.90$ and $F(7, 84) = 15.39$, and for the interaction, $F(24, 288) = 3.47$ and $F(21, 252) = 3.16$, respectively, all $p < 0.01$.

The right panel of Figure 3 is a sharp contrast to the left panel, which shows flat functions within each scale and discrete steps between scales. In the right panel, log roughness tends to increase with log ridge width within each scale and the data from the different scales appear to collapse onto a single function. To confirm these observations, linear functions were fit within each level of groove width. The slopes and intercepts are shown for each scale in Figure 4. When the 95% confidence intervals around each mean slope were computed, four of the five functions—all but the one from the largest scale—had intervals that excluded zero. The fact that the largest slope was not different from zero indicates, as was found before, that the effect of ridge width on perceived roughness saturates at high levels of ridge width.

Table I. Mean and Standard Deviation of Kinematic Variables by Experiment

Experiment	Speed-x (mm/s)	Speed y (mm/s)	y Std Dev (mm)	Duration (s)
1	54.3 (3.1)	16.6 (1.2)	3.0 (0.2)	5.3 (0.6)
2	64.3 (3.5)	20.3 (1.2)	2.6 (0.2)	5.0 (0.6)
3	70.0 (3.2)	27.6 (1.4)	3.8 (0.3)	5.4 (0.9)

Table II. Significant ($p < 0.05$) Correlations of Kinematic Variables with Stimulus Variables and Log Perceived Roughness by Experiment

Experiment		Speed x	Speed y	Duration	y Std Dev
1	Log ridge width		0.593	0.845	0.695
	Log groove width	0.544	0.611	0.784	0.592
	Log spatial period	0.379	0.629	0.850	0.674
	Log perceived roughness		0.630	0.868	0.716
	Ridge:groove	−0.602			
2	Log ridge width	0.403	0.413	0.663	0.635
	Log groove width	0.762		0.594	0.580
	Log spatial period	0.661	0.326	0.645	0.625
	Log perceived roughness	0.401	0.337	0.565	0.503
	Ridge:groove	−0.798			
3	Log ridge width			0.792	0.812
	Log groove width	0.613		0.775	0.779
	Log spatial period	0.482		0.818	0.823
	Log perceived roughness			0.732	0.806
	Ridge:groove	−0.518			

All of the zero-intercept values were significantly greater than zero and they did not differ significantly from one another, $F(4, 48) < 1$, supporting the idea that the local functions fit within scales lay on the same global trend line. However, the global function relating roughness to all ridge width values appears not to be entirely linear, as there was a significant trend for the slopes of the local functions to decrease as scale (groove width) increased, $F(1, 48) = 11.65$, $p < 0.01$. Thus, as in Experiments 1 and 2, ridge width was found to have a decreasing effect as groove width increased. Equivalently, since groove width and spatial period covary, one could say that the effect of ridge width decreased as spatial period increased.

6. RESULTS OF KINEMATIC VARIABLES IN ALL EXPERIMENTS

The mouse x and y position values (frontal and sagittal, respectively) were sampled at 50 Hz. To measure the kinematics of exploration, pauses of greater than 100 ms were eliminated from the data. The kinematic measures are speed in the x and y direction (total pixels moved, divided by duration, excluding pauses, converted to mm/s), the total duration of exploration (excluding pauses), and the standard deviation of position along the y axis, which indicates the tendency of subjects to move the mouse parallel to the grating, e.g., by moving in a circle. (Note that duration is strongly correlated with other measures of the extent of exploration in the x direction, e.g., the number of reversals along the x axis and with the number of pauses longer than 100 ms. Among these redundant variables, we focus only on duration.)

Means and standard deviations across subjects of the kinematic variables are shown in Table I. Table II shows the significant correlations of kinematic variables with geometric variables describing the stimulus and with log roughness, where the units of observation are the surfaces for the given experiment; each observation is the mean across subjects for a given surface. The geometric variables are log ridge size, log groove size, log spatial period, and ridge:groove ratio.

There are three general observations from the kinematic analysis: (1) Greater resistive area tended to slow exploration. This is indicated by finding that speed in the x direction was negatively related to ridge:groove ratio and positively related to groove width. As expected, given that the resistance varied only along the x axis, the speed in the y direction was not consistently related to geometric variables, although some correlations were significant. (2) As textural patterns grew larger on either dimension, exploration took longer and deviated more along the y axis. This is indicated by the fact that both the duration of movement and y deviation were positively related to ridge and groove width and to spatial period. (3) Surfaces that were perceived as rougher were explored more extensively. Thus roughness magnitude was positively related to both the duration of the movement and deviation into the y direction. This association between roughness and extent of exploration is undoubtedly mediated by the effects of resistance on both these variables. That is, exploration increases with resistance and so does roughness.

7. GENERAL DISCUSSION

The present experiments demonstrate that resistive variations on a surface can reliably lead to a sensation of roughness. The pattern observed across all three experiments was for roughness to increase with the size of the resistive ridge. The effects of groove width were small and inconsistent. Therefore, any effects of spatial period were mediated by larger ridge widths.

Two questions to consider about the subjective magnitudes are (a) whether what the subject experienced is appropriately called roughness, and (b) whether the experience was uniform across the range of stimuli. With respect to the first question, we can only say that our subjects were willing to characterize variations across the stimulus array as different roughness values. Without instructions as to how to think of the stimuli (going over bumps in the road), however, pilot subjects sometimes professed uncertainty as to how to perform the roughness ratings. Similar uncertainty has been found for textures that are explored with the bare finger, once interelement spacing becomes large (∼3.5 mm) and geometry becomes salient.

With regard to the second question, Seungmoon Choi [personal communication 2005] suggested to us that the subjective roughness of a virtual texture acts quite nonuniformly across different spatial periods. When the spatial period is large, the texture can be construed geometrically as well as intensively. As spatial period decreases, there is a stage in which there is a strong sense of roughness, but geometry cannot be resolved. Finally, at low spatial periods, users feel a general impression of roughness, but it is essentially invariant over any further changes in the stimulus. The cut points for these impressions would vary with exploratory factors, such as, velocity and with device characteristics. This characterization may help to explain why we did not find significant effects of variations in ridge:groove within the smallest spatial periods in Experiment 1, despite our tests indicating that the device was at least marginally capable of rendering these differences.

The form of the magnitude-estimation function obtained here is quite different from previous psychophysical studies. Log roughness was essentially invariant over log groove width. This sharply contrasts with the power-law increase commonly found when people explore with the bare finger [Lederman 1974] and with the quadratic trend that has been found when they explore with rigid probes [e.g., Klatzky et al. 2003]. The results also depart from recent work with force-feedback devices that indicates roughness magnitude decreases with groove width [Penn et al. 2003] and with findings in our companion paper [Lederman et al. 2006].

In all three experiments here, the effects of ridge width appeared to saturate at high levels. One can estimate a ridge of 1.25 mm as an upper bound on the saturation point, on the basis of Experiment 2, where roughness did not differ between ridge widths of 0.62 and 1.25 mm. Examination of Figures 2 and 3 (right panel) are consistent with this estimate, in that they indicate that increases in ridge width beyond 1.25 mm had no effect on perceived roughness. We assume that the saturation point would depend on the sliding friction and viscosity parameters that govern the resistance. Further work will be necessary to test this assumption.

By saying that roughness increases with ridge width, we mean that it is related to the duration or spatial extent of an uninterrupted period of resistance. This is not to be confused with measures that normalize ridge width. Three normalized alternatives might be considered. (1) One might propose that roughness is related to ridge width relative to groove width, or the ridge:groove ratio. This can be ruled out by Experiment 2, where there was no effect of groove width when ridge width was held constant. This means that neither ridge:groove ratio nor ridge relative to spatial period (sum of ridge and groove widths) is the determining factor for perceived roughness. (2) One might propose that the perceptual system, when computing roughness, takes into account the proportion of exploration that encounters resistance. To test this, we correlated log roughness with the proportion of time subjects spent on ridges, calculated as $D * R/S$, where D = duration of exploration, R = ridge width, and S = spatial period. The correlations across stimulus surfaces were not consistently strong ($r = 0.29, 0.11$, and 0.56 for Experiments 1–3, respectively, *dfs* = 36, 38, and 37, only the last reaching significance, $p < 0.05$). (3) A similar proposal is that roughness is sensitive to the proportion of distance traveled that was spent on ridges. This formulation is equivalent to the preceding expression, except that the duration of exploration is replaced with the product of duration and speed. The correlations with roughness were stronger, but did not account for substantial variance ($r = 0.37, 0.20$, and 0.61, for Experiments 1–3, respectively, the first and third reaching $p < 0.05$).

Our findings further indicate that using one-DoF resistance as a cue to roughness is quite different from using vibration. Consider that the fundamental vibratory frequency can be estimated by the speed of travel, divided by the spatial period. Because spatial period is the sum of ridge and groove widths, vibratory frequency accordingly should decrease as ridge width increases. Empirically, however, roughness *increases* as ridge width increases. Given the empirical finding, a mediating effect of ridge width on vibration should lead to a negative relationship between vibratory frequency and roughness. Indeed, the estimate of vibratory frequency (i.e., speed divided by spatial period) was strongly correlated negatively with log roughness ($r = -0.70, -0.78$, and -0.92, for Experiments 1–3, respectively; all $p < 0.05$).

Our data suggest, then, that when subjects rub a probe across resistive patches, their sense of roughness is based on the resistance within each single, integral patch. The perceptual system underlying this percept seems relatively insensitive to the duration of pauses in the resistance (i.e., grooves). Therefore the receptor populations that are involved likely provide sustained responses. They could include the slowly adapting cutaneous receptors and other receptors in muscles, tendons, and joints. The receptor responses, we suggest, are integrated over a continuous period of relatively high resistance and are fed into a process that computes the roughness response. This process apparently saturates once the resistive patch exceeds some limit in time or space. We estimate the spatial limit, under the current parameterization and device, to be within 1.25 mm.

The process we are describing is quite different from models of roughness perception with 3D surfaces felt via the bare finger or through a rigid probe, as were described in the introduction. Although resistance-based roughness, as rendered with the present device, appears to be under the control of different factors, our data indicate that people do have a reliable perceptual response. These results suggest, then, that a resistance algorithm could be useful in a variety of applications. An advantage for using resistive textures in applied settings is that they can be supplied with inexpensive, highly portable devices. The Logitech force-feedback mouse, although not currently in manufacture, was marketed inexpensively. A similar device might potentially be used to enhance the sense of presence in a wide range of applications, such as teledermatology and electronic commerce. Its potential, we believe, merits further study.

ACKNOWLEDGMENTS

We thank Robert H. Swendsen for designing the experiments to determine the mouse resistance parameters and Sara Langseth for data collection and analysis. We also thank Immersion Corp. for donating the mouse and Chris Hasser, Dean Chang, and Bruce Schena for supplying information on its performance parameters.

APPENDIX

To characterize the resistance generated by the mouse, we performed tests in which the mouse was programmed to respond to an attractor force along the x axis for a period of approximately 100–150 ms; the mouse position was sampled at 67 Hz. The surface resistance was set to the parameters of either the ridge or the groove and the attractor force level was varied across runs. The metric of this force is set by Logitech.

The first test was conducted with the groove surface. There were two runs at each of four force levels. The mouse x position over time was very well fit in each case by a parabola. The acceleration, as determined from the quadratic term of the parabola and averaged over the 2 runs, was a linear function of force, $r^2 = 0.997$. From this function, using Eq. (1) below, we derived estimates of the sliding friction coefficient, μ, and the calibration factor between the manufacturer's force metric (f) and the conventional Newton metric (N) (estimated as $N = 0.0003{*}\mathrm{f}$).

The second test was conducted with the ridge surface. There were three runs at each of nine force levels. In all cases, the acceleration was essentially constant, indicating the viscosity component, γ, was positive. A function relating the average velocity during a run to force was highly linear, $r^2 = 0.990$. From this function we derived a second estimate of μ and an estimate of the viscosity factor, γ.

Based on these tests, we characterize the mouse by the parameters given below. It should be noted that these parameter estimates are subject to trial-to-trial variability and also have been found to vary as the mouse warms up with use. We, therefore, suggest them as approximations only. The equation is:

$$F - \mu^* m^* g - \gamma^* v = m^* a \tag{1}$$

where m is the mouse mass (measured at 0.12 kg), g is gravitational acceleration, $\mu = 0.5$, γ is 0 for the groove, and 0.01 N-s/mm for the ridge.

Given the average speeds in Table I and noting that subjects moved more slowly on ridges, we estimate that they encountered about 0.6 N total force on a groove and 1 N on a ridge. This is commensurate with the device developers' estimates of its capabilities for force generation.

In a third test, we measured the static coefficient of friction by determining the minimum force that, when applied, would cause the mouse to slide. For both ridge and groove, the static coefficient was estimated as 0.9.

REFERENCES

Campion, G. and Hayward, V. 2005. Fundamental limits in the rendering of virtual haptic textures. *Proceedings of the 1st Joint Eurohaptics Conference and Symposium on Haptic Interfaces for Virtual Environment and Teleoperator Systems*. IEEE Computer Society, Los Alamitos, CA. 263–270.

Choi, S. and Tan, H. Z. 2002. An analysis of perceptual instability during haptic texture rendering. *Proceedings of the 10th International Symposium on Haptic Interfaces for Virtual Environment and Teleoperator Systems*. IEEE Computer Society, Los Alamitos, CA. 1261–1268.

Choi, S. and Tan, H. Z. 2003. An experimental study of perceived instability during haptic texture rendering: Effects of collision detection algorithm. *Proceedings of the 11th International Symposium on Haptic Interfaces for Virtual Environment and Teleoperator Systems*. IEEE Computer Society, Los Alamitos, CA. 197–204. :

Colwell, C., Petrie, H., Kornbrot, D., Hardwick, A., and Furner, S. 1998. Use of a haptic device by blind and sighted people: Perception of virtual textures and objects. Presented at *Third TIDE Congress Technology for Inclusive Design and Equality*, Helsinki, Finland.

Drewing, K., Ernst, M.O., Lederman, S. J., and Klatzky, R. L. 2004. Roughness and spatial density judgments on visual and haptic textures using virtual reality. Presented at *Euro-Haptics Conference, Munich, Germany*.

Ho, P. P., Adelstein, B. D., and Kazerooni, H. 2004. Judging 2D versus 3D square-wave virtual gratings. *Proceedings of the 12th International Symposium on Haptic Interfaces for Virtual Environment and Teleoperator Systems*. IEEE Society, Los Alamitos, CA. 176–183.

Jansson, G. 1998. Can a haptic force feedback display provide visually impaired people with useful information about texture, roughness and 3-D form of virtual objects? Presented at *2nd European Conference on Disability, Virtual Reality, and Associated Technologies*, Skovde, Sweden.

Klatzky, R. L. and Lederman, S. J. 1999. Tactile roughness perception with a rigid link interposed between skin and surface. *Perception and Psychophysics, 61*, 591–607.

Klatzky, R. L. and Lederman, S. J. 2002. Perceiving texture through a probe [chapter 10]. In *Touch in Virtual Environments*, M. L. McLaughlin, J. P. Hespanha, and G. S. Sukhatme, Eds. Prentice Hall, Upper Saddle River, NJ. 180–193.

Klatzky, R. L., Lederman, S. J., Hamilton, C., Grindley, M., and Swendsen, R. H. 2003. Feeling textures through a probe: Effects of probe and surface geometry and exploratory factors. *Perception and Psychophysics, 65*, 613–631.

Lederman, S. J. 1974. Tactile roughness of grooved surfaces: The touching process and effects of macro- and microsurface structure. *Perception and Psychophysics, 24*, 154–160.

Lederman, S. J. 1983. Tactual roughness perception: Spatial and temporal determinants. *Canadian Journal of Psychology, 37*, 498–511.

Lederman, S. J., Klatzky, R. L., Hamilton, C. L., and Ramsay, G. I. 1999. Perceiving roughness via a rigid probe: Psychophysical effects of exploration speed and mode of touch. *Haptics-e, The Electronic Journal of Haptics Research*, *1*, 1.

Lederman, S. J., Klatzky, R. L., Hamilton, C., and Grindley, M. 2000. Perceiving surface roughness through a probe: Effects of applied force and probe diameter. *Proceedings of the ASME Dynamic Systems and Control Division, DSC-Vol. 69-2*. 1065–1071.

Lederman, S. J., Klatzky, R. L., Tong, C., and Hamilton, C. L. 2006. The perceived roughness of resistive virtual textures: II. Effects of varying viscosity with a force-feedback device. *ACM Transactions on Applied Perception*, *3*, 1, 15–30.

Massie, T. H. 1996. Initial haptic explorations with the PHANTOM: Virtual touch through point interaction. Ph.D. thesis, Massachusetts Institute of Technology, Cambridge, MA.

Minsky, M. D. R. 1995. Computational haptics: The sandpaper system for synthesizing texture for a force-feedback display. Ph.D. thesis, Massachusettts Institute of Technology, Cambridge, MA.

Minsky, M. D. R. and Lederman, S. J. 1996. Simulated haptic textures: Roughness. *Proceedings of the ASME Dynamic Systems and Control Division 58*. 421–426.

Okamura, A. M., Dennerlein, J. T., and Howe, R. D. 1998. Vibration feedback models for virtual environments. *Proceedings of the IEEE International Conference on Robotics and Automation 1*. 674–679.

Otaduy, M. A. and Lin, M. C. 2004. A perceptually-inspired force model for haptic texture rendering. *Proceedings of the 1st Symposium on Applied Perception in Graphics and Visualization 1*. 123–126.

Penn, P., Kornbrot, D., Furner, S., Hardwick, A., Colwell, C., and Petrie, H. 2003a. Roughness perception in haptic virtual reality: The impact of the haptic device, endpoint and visual status. Unpublished manuscript.

Penn, P., Kornbrot, D., Furner, S., Hardwick, A., and Petrie, H. 2003b. The effect of contact force on roughness perception in haptic virtual reality. Unpublished manuscript.

Siira, J. and Pai, D. K. 1996. Haptic texturing—A stochastic approach. In *Proceedings of the IEEE International Conference on Robotics and Automation*, IEEE Computer Society, Los Alamitos, CA. 557–562.

Wall, S. A. and Harwin, W. S. 1999. Modeling of surface identifying characteristics using Fourier series. *Proceedings of the ASME Dynamic Systems and Control Division 67*. 65–71.

Weisenberger, J. M., Krier, M. J., and Rinker, M. A. 2000. Judging the orientation of sinusoidal and square-wave virtual gratings presented via 2-DOF and 3-DOF haptic interfaces. *Haptics-e, The Electronic Journal of Haptics Research 1*. 1–20.

Received March 2005; revised August 2005; accepted November 2005